

# A method for skin malformation classification by combining multispectral and skin autofluorescence imaging

*I. Lihacova<sup>\*a</sup>, K. Bolochko<sup>b</sup>, E. V. Plorina<sup>a</sup>, M. Lange<sup>a</sup>, I. Oshina<sup>a</sup>, A. Lihachev<sup>a</sup>*

<sup>a</sup>University of Latvia, Institute of Atomic Physics and Spectroscopy, Riga, Latvia, LV1050

<sup>b</sup>Riga Technical University, Faculty of Computer Science and Information Technology, Riga, Latvia, LV1048

*\*ilze.lihacova@lu.lv*

## Abstract

In this study we combined multispectral  $p'$  imaging and skin autofluorescence methods using self-made prototype with 4 LED illumination- 405 nm, 526 nm, 663 nm and 964 nm. Described method was tested on 6 skin lesion groups: melanomas (3 histologically confirmed cases), seborrheic keratosis (13 dermatologically confirmed cases), hyperkeratosis (8 histologically and 1 dermatologically confirmed cases), melanocytic nevi (23 dermatologically confirmed cases), basal cell carcinomas (2 histologically and 16 dermatologically confirmed cases) and hemangiomas (8 dermatologically confirmed cases). With this method we achieved 100% sensitivity and 100% specificity for distinguishing melanoma from the rest lesion groups. Unfortunately, with this method it is impossible to separate basal cell carcinomas from benign lesions.

## Equipment

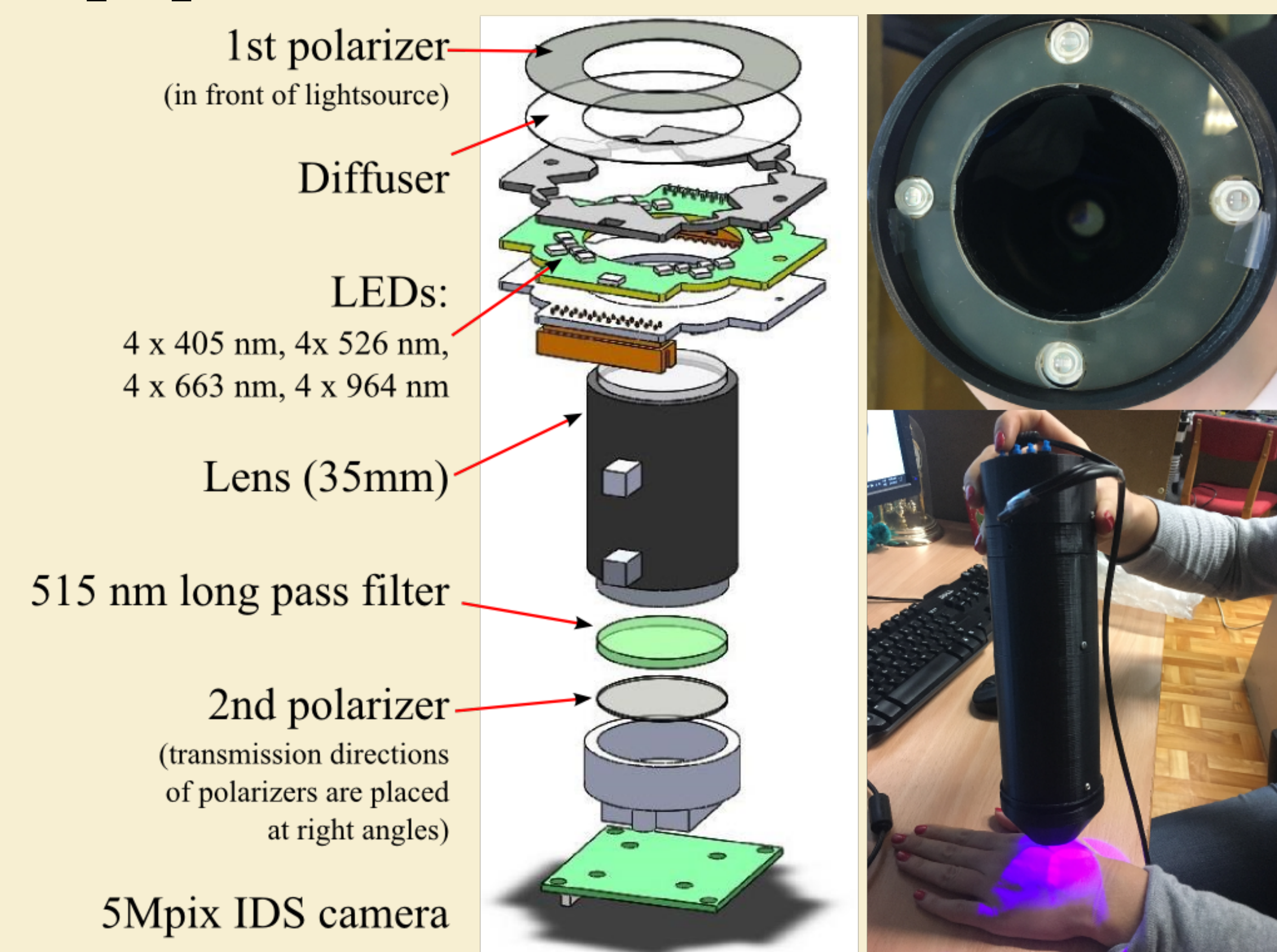


**Fig. 1.** The prototype for data acquisition. Device consists of 4 x 405 nm, 4 x 526 nm, 4 x 663 nm, 4 x 964 nm LEDs, 2 linear polarizers placed at right angles, diffuser, 515 nm long pass filter, 5 Mpix IDS camera.

## Method

The proposed method is a combination of two pre-developed techniques [1] and [2].

### 1. Multispectral $p'$ imaging method

In this study we simplified the previously developed method for OD image processing [1]. For calculations we obtained images of lesion and healthy skin at 4 different wavelength illumination. Healthy skin was measured as close to the lesion as possible. For  $p'$  map calculations we used modified formula for our specific prototype with specific wavelengths close to method described earlier [1]:

$$p' = \lg \left( \frac{I(526) \cdot I_{skin}(663) \cdot I_{skin}(964)}{I_{skin}(526) \cdot I(663) \cdot I(964)} \right)$$

where  $I(526)$ ,  $I(663)$  and  $I(964)$  are reflection images from lesion at 526 nm, 663 nm, and 964 nm illumination;  $I_{skin}(526)$ ,  $I_{skin}(663)$ , and  $I_{skin}(964)$  are reflection images from healthy skin near the lesion at 526 nm, 663 nm, and 964 nm illumination. Exposure time for each illumination and each case was chosen to avoid overexposed pixels and values equal to 0. It is important that each pair of  $I(\lambda)$  and  $I_{skin}(\lambda)$  at particular illumination has been captured at the same exposure time.

To get the results, the region of interest in  $p'$  map within the lesion was marked manually using the MatLAB software. The maximal possible region within lesion was selected using rectangular markup tool. The mean of 100 highest values from the selected area (mean  $p'_{max}$ ) was calculated.

### 2. Skin autofluorescence imaging method

For the skin autofluorescence excitation the 405 nm LEDs were used. Prototype was placed on the area of interest, then the 405 nm LED was switched on and the image was captured. Lesion images were captured with 400 ms exposure time. The obtained RGB image represents spatial distribution of AF intensity in the spectral region from 515 nm to 700 nm. To create a diagnostic parameter, the mean intensity was calculated from RGB image G-band for each lesion using MatLAB software. The lesion areas were marked manually within the lesion with broken lines. The boundary of lesion was determined visually. The border was identifying by changes in intensity compared to the surrounding healthy skin.

## Results

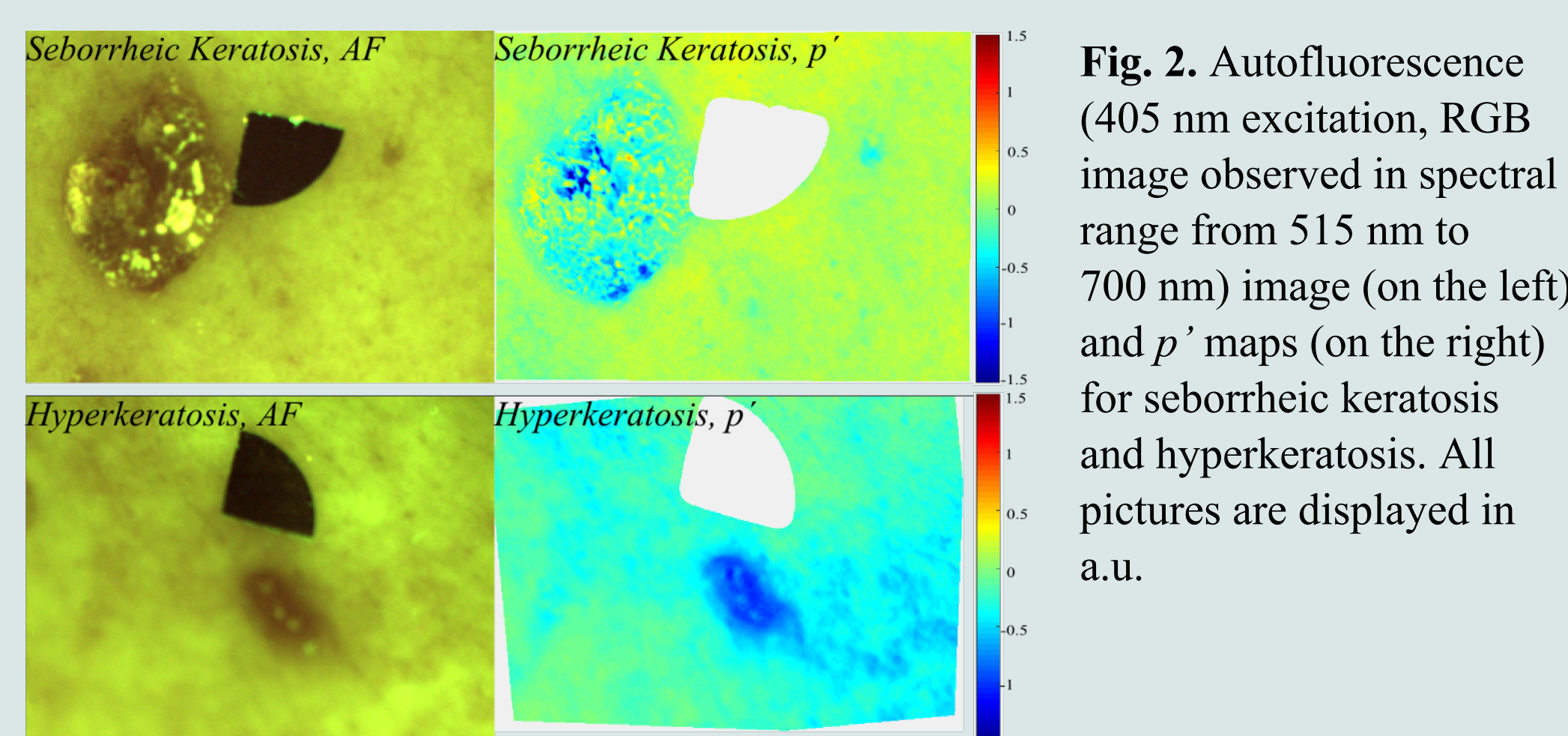


**Fig. 2.** Autofluorescence (405 nm excitation, RGB image observed in spectral range from 515 nm to 700 nm) image (on the left) and  $p'$  maps (on the right) for seborrheic keratosis and hyperkeratosis. All pictures are displayed in a.u.

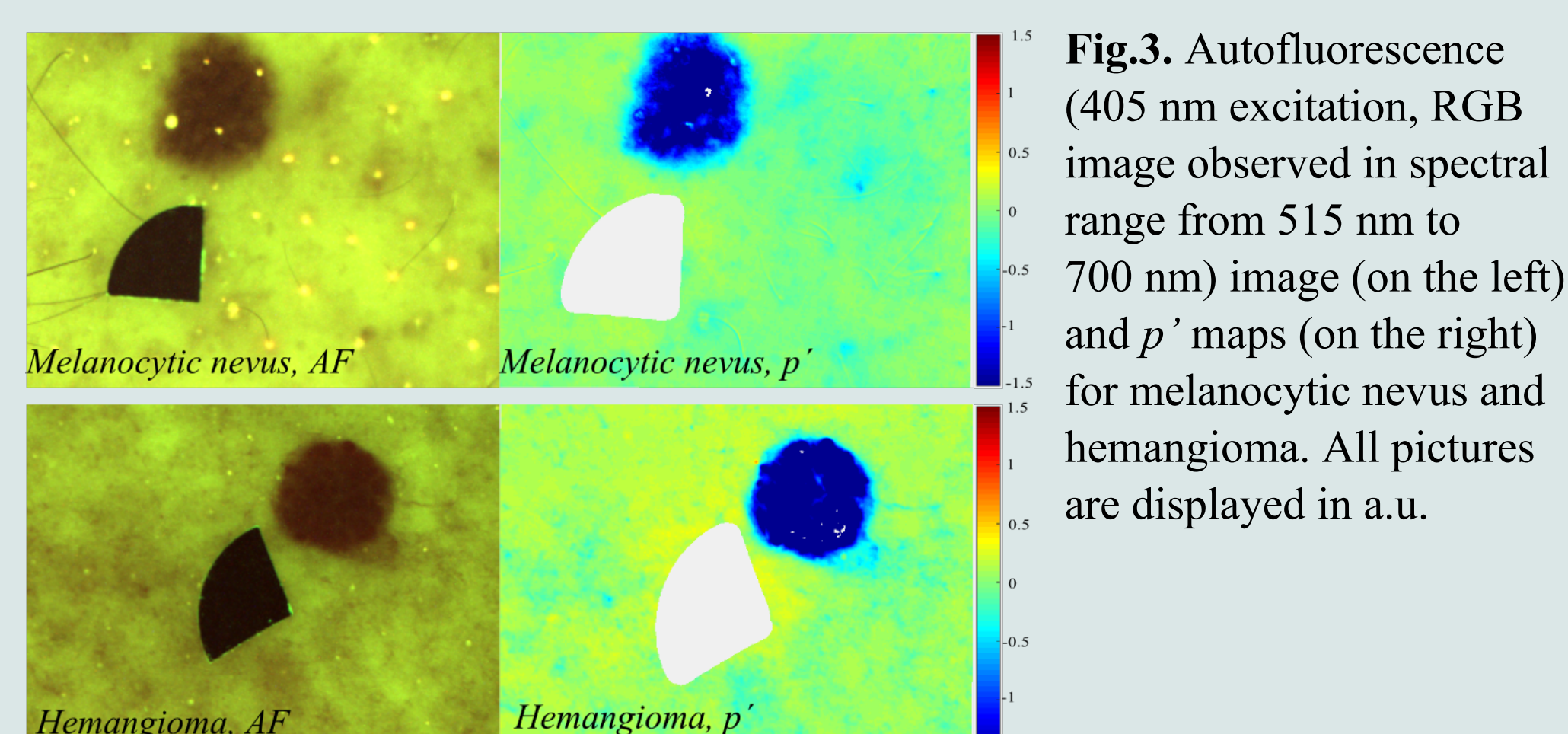


**Fig. 3.** Autofluorescence (405 nm excitation, RGB image observed in spectral range from 515 nm to 700 nm) image (on the left) and  $p'$  maps (on the right) for melanocytic nevus and hemangioma. All pictures are displayed in a.u.

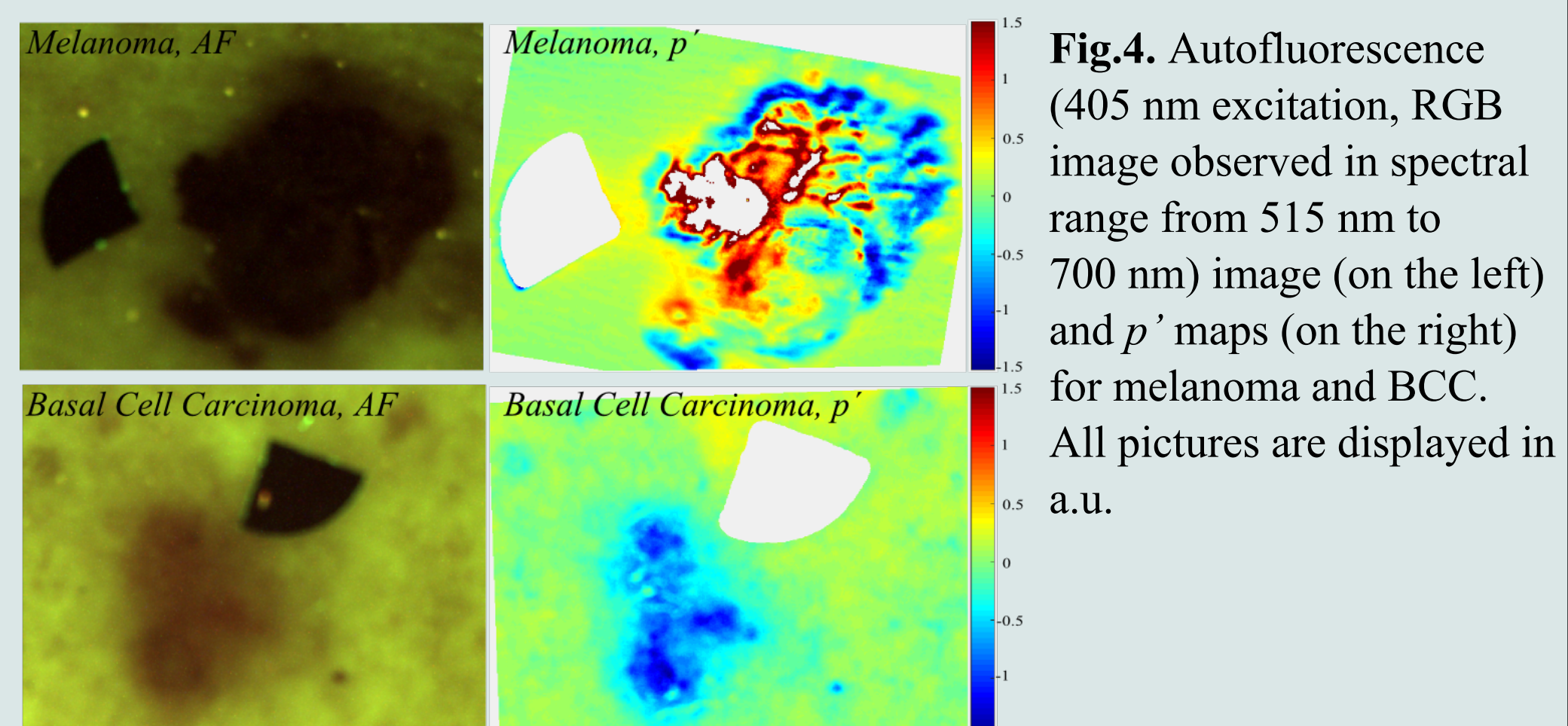


**Fig. 4.** Autofluorescence (405 nm excitation, RGB image observed in spectral range from 515 nm to 700 nm) image (on the left) and  $p'$  maps (on the right) for melanoma and BCC. All pictures are displayed in a.u.

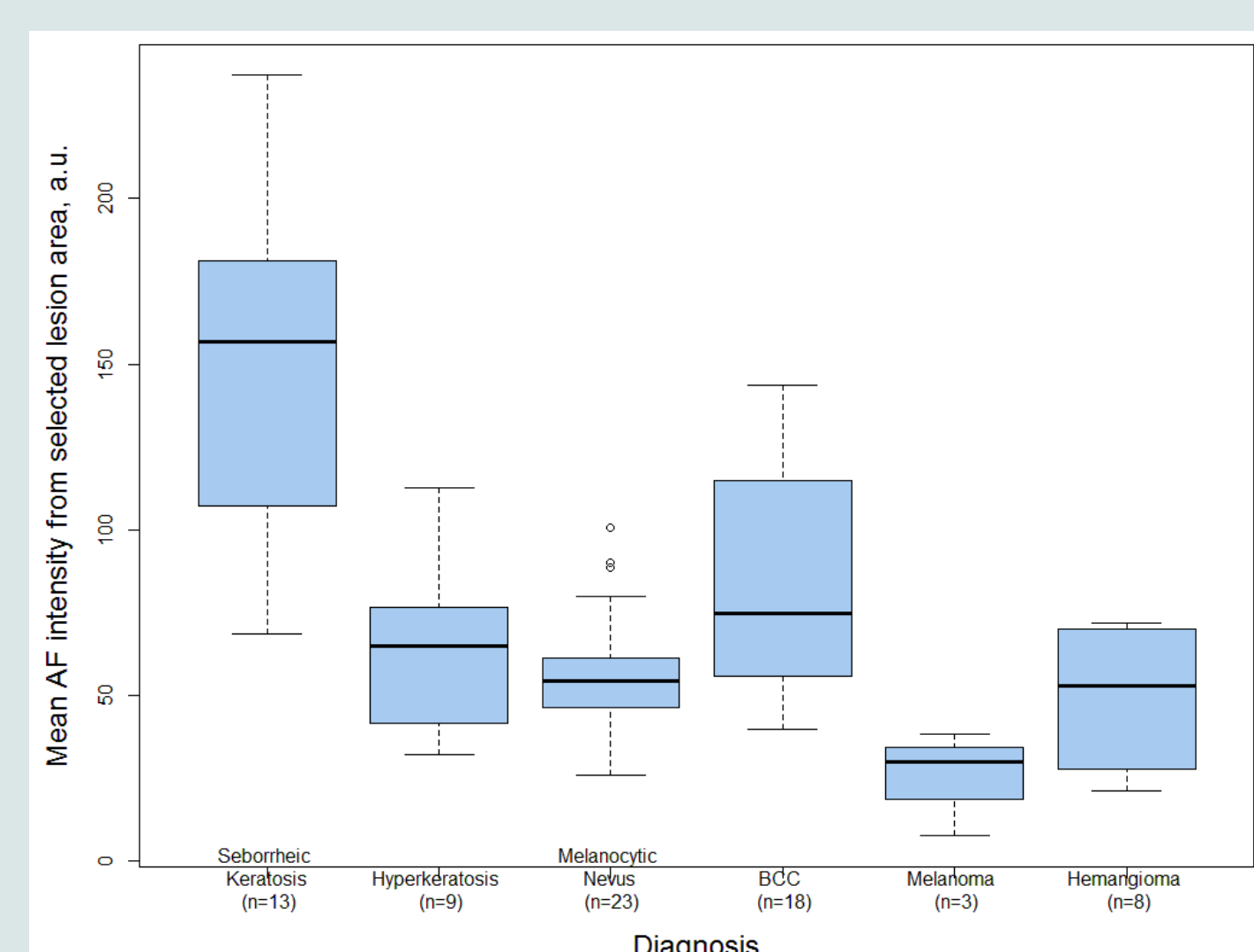


**Fig. 5.** Box-whisker plot of mean AF intensity from selected lesion area for different lesion groups.

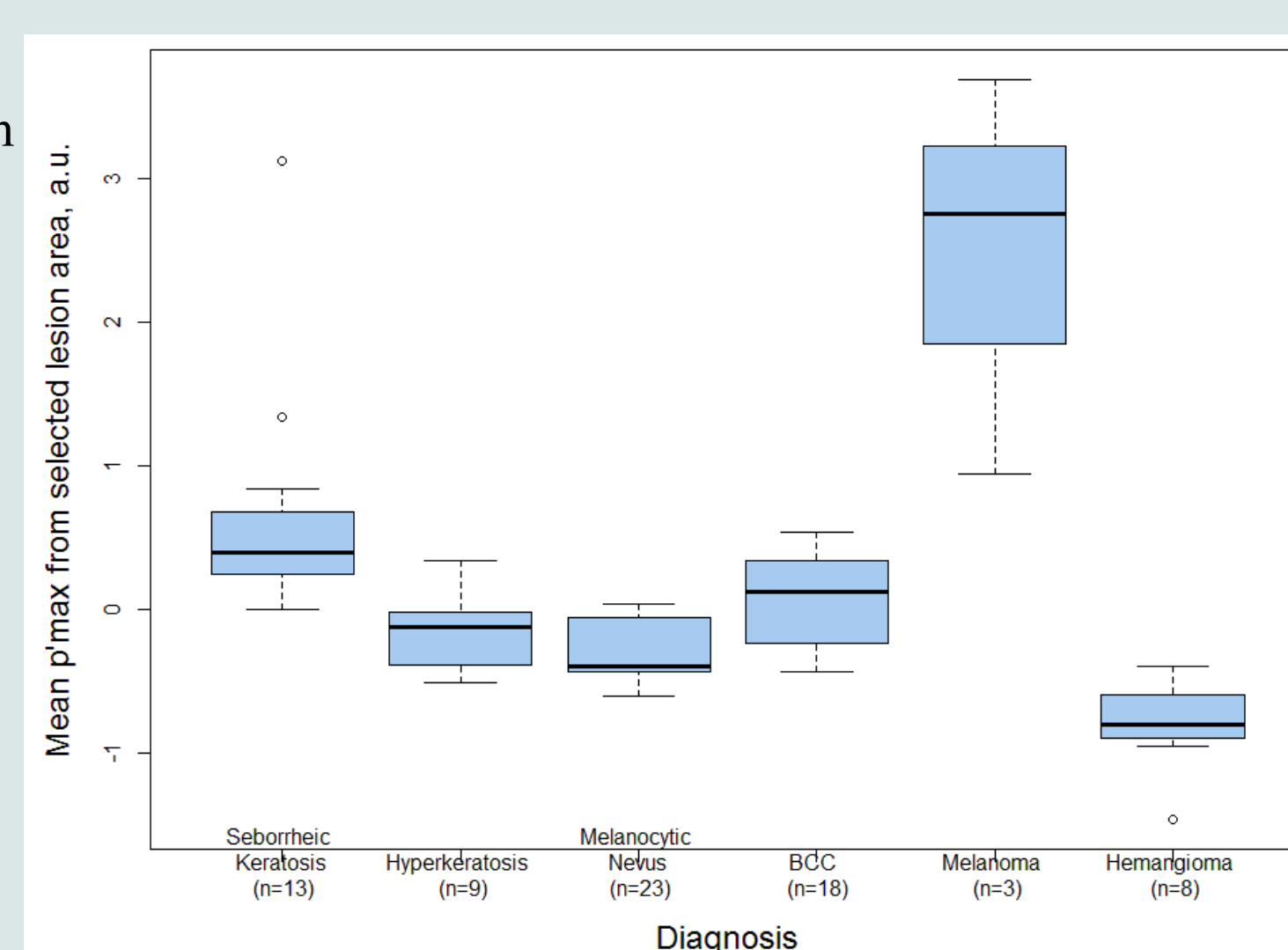


**Fig. 6.** Box-whisker plot of mean  $p'_{max}$  (estimated from 100 maximal values) from selected lesion area for different lesion groups.

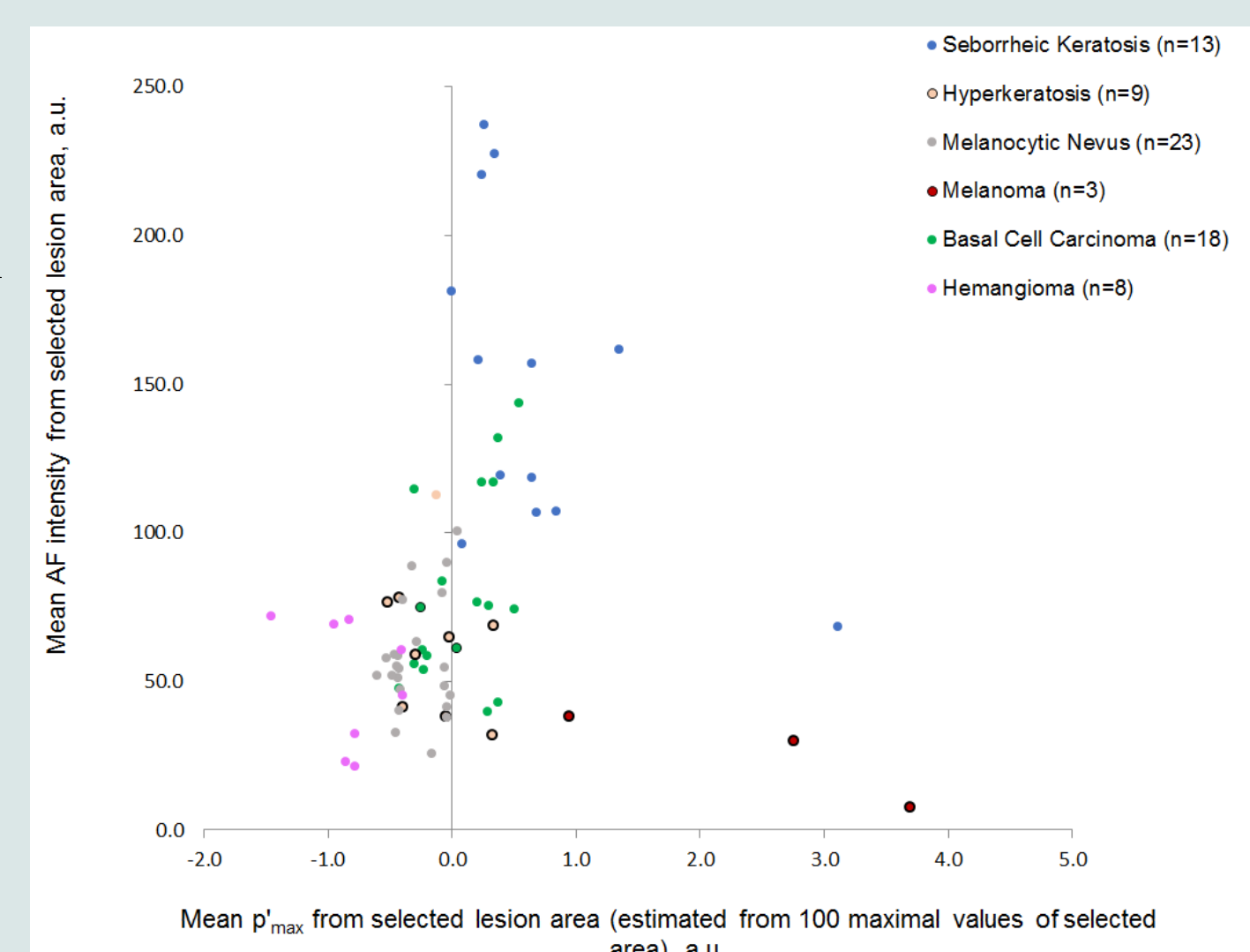


**Fig. 7.** Mean AF intensity from selected lesion area vs. mean  $p'_{max}$  from selected lesion area (estimated from 100 maximal values of selected area). Histologically validated diagnoses are denoted with black circle around marker.

## Summary and Discussion

The presented study combines two imaging modalities of in-vivo skin: autofluorescence imaging under 405 nm LED excitation and multispectral reflectance imaging under 526 nm, 663 nm, and 964 nm LED illumination. For the clinical measurements a custom designed prototype was used. Combining these methods, the criterion was set: mean  $p'_{max} > 0.9$  a.u. mean  $AF < 50$  a.u. Using this criterion, we calculated that it is possible to discriminate melanomas from other lesion groups (seborrheic keratosis, hyperkeratosis, melanocytic nevi, BCC and hemangiomas) with sensitivity 100% and specificity 100%. However, only 3 melanomas data have been used in these calculations. Nevertheless, previous  $p'$  map calculations for 30 melanoma data, using OD images [1, 3], indicated a high potential for the separation of melanomas from other pigmented lesions. We expect that further melanoma data could show a similar trend as described in this article. By combining the  $p'$  imaging with AF method it is possible to add seborrheic keratosis and hyperkeratosis groups and successfully distinguish them from melanomas. Unfortunately, currently this method is not sensitive to unpigmented BCC.

## Conclusions

By combining  $p'$  imaging with skin AF method, we obtained 100% sensitivity and 100% specificity for melanoma discrimination from seborrheic keratosis, hyperkeratosis, melanocytic nevi, BCC and hemangiomas. In order to use this method in practice, it would be necessary to obtain more melanoma data. This method is applicable for melanoma diagnostics. Adding the criterion that distinguishes BCC from benign skin lesions, it has a great potential to be used in primary care physicians' practice.

## References

- [1] I. Diebele et al., "Clinical evaluation of melanomas and common nevi by spectral imaging," Biomed. Opt. Express 3(3), 467-472 (2012).
- [2] A. Lihachev et al., "Differentiation of seborrheic keratosis from basal cell carcinoma, nevi and melanoma by RGB autofluorescence imaging," Biomed. Opt. Express 9(4), 1852-1858 (2018).
- [3] I. Lihacova et al., "Semi-automated non-invasive diagnostics method for melanoma differentiation from nevi and pigmented basal cell carcinomas," Proc. SPIE 10592, Biophotonics—Riga 2017, 1059206 (2017).

## Acknowledgments

This work has been supported by two European Regional Development Fund projects: "Development and clinical validation of a novel cost effective multi-modal methodology for early diagnostics of skin cancers" (No. 1.1.1.2/16/I/001, agreement No. 1.1.1.2/VIAA/1/16/052) and "Portable Device for Non-contact Early Diagnostics of Skin Cancer" (No. 1.1.1.1/16/A/197).